From Multi-Risk Evaluation to Resilience Planning: The Case of Central Chilean Coastal Cities

**Pilar Barría [1,2,*], María Luisa Cruzat [3], Rodrigo Cienfuegos [1,3], Jorge Gironás [1,3,4,5],
Cristián Escauriaza [1,3], Carlos Bonilla [3,4], Roberto Moris [6], Christian Ledezma [7],
Maricarmen Guerra [3,8], Raimundo Rodríguez [9] and Alma Torres [6]**

[1] Centro de Investigación para la Gestión Integrada de Desastres Naturales, Conicyt/Fondap/15110017, Santiago 7820436, Chile; racienfu@ing.puc.cl (R.C.); jgironas@ing.puc.cl (J.G.); cescauri@ing.puc.cl (C.E.)

[2] Departamento de Gestión Forestal y su Medio Ambiente, Facultad de Ciencias Forestales y de la Conservación de la Naturaleza, Universidad de Chile, Santiago 8820808, Chile

[3] Departamento de Ingeniería Hidráulica y Ambiental, Pontificia Universidad Católica de Chile, Santiago 7820436, Chile; mluisacruzats@gmail.com (M.L.C.); cbonilla@ing.puc.cl (C.B.); mnguerra@uc.cl (M.G.)

[4] Centro de Desarrollo Urbano Sustentable, CONICYT/FONDAP/15110020, Santiago 7530092, Chile

[5] Centro Interdisciplinario de Cambio Global, Pontificia Universidad Católica de Chile, Santiago 7820436, Chile

[6] Instituto de Estudios Urbanos y Territoriales, Pontificia Universidad Católica de Chile, Santiago 7530091, Chile; rmoris@uc.cl (R.M.); adtorres@uc.cl (A.T.)

[7] Departamento de Ingeniería Estructural y Geotécnica, Pontificia Universidad Católica de Chile, Santiago 7820436, Chile; ledezma@ing.puc.cl

[8] Applied Physics Laboratory, University of Washington, Seattle, WA 98105, USA

[9] Edic Ingenieros, Santiago 7560873, Chile; raimundorodriguezt@gmail.com

* Correspondence: pbarria@uchile.cl; Tel.: +56-2-2978-5945

check for updates

Abstract: Multi-hazard evaluations are fundamental inputs for disaster risk management plans and the implementation of resilient urban environments, adapted to extreme natural events. Risk assessments from natural hazards have been typically restricted to the analysis of single hazards or focused on the vulnerability of specific targets, which might result in an underestimation of the risk level. This study presents a practical and effective methodology applied to two Chilean coastal cities to characterize risk in data-poor regions, which integrates multi-hazard and multi-vulnerability analyses through physically-based models and easily accessible data. A matrix approach was used to cross the degree of exposure to floods, landslides, tsunamis, and earthquakes hazards, and two dimensions of vulnerability (physical, socio-economical). This information is used to provide the guidelines to lead the development of resilience thinking and disaster risk management in Chile years after the major and destructive 2010 Mw8.8 earthquake.

Keywords: multi-risk matrix; resilience; flood risk; multi-hazard; risk reduction

1. Introduction

Deficient urban planning together with a lack of integrated disaster risk management plans may result in important economic and social costs for a community [1]. The continuous population growth, the major growth and urban development trend of coastal cities during the last decades [2], the unregulated urban immigration along with climate change induced extreme hydroclimatic events [3], are likely to strengthen geo-risks derived from natural hazard [1]. Particularly concerning is the case of port cities that concentrate most of the world commercial trade, tourism, and recreation activities [4]. These factors impact what are considered to be the three components interacting to

explain disaster risks: the threatening physical phenomena—hazard; the population, infrastructure, economic, and social assets exposed to the hazard—exposure; and the predisposition of society to deal with the event—vulnerability [1,5–7].

The Intergovernmental Panel on Climate Change (IPCC) highlights that suitable methodologies to evaluate the different risk components depend on the local decision-making context, and include qualitative and quantitative approaches [1]. An appropriate risk evaluation methodology for a given region should effectively provide the information about the physical and social-environmental characteristics needed to reduce the risk and to increase resilience through the design and application of disaster risk management plans. Although several studies have investigated disaster risk evaluations worldwide, two limitations are still identified: (1) different hazard events threatening the same region are typically not integrally assessed (e.g., [8,9]), and (2) these studies do not comprehensively contemplate the complexity of all the components that define the risk (e.g., [10,11]), which may result in an underestimation of risk. Thereby, multi-risk approaches, which involve the analysis of multiple hazards and their interactions with exposure and vulnerability are an active area of research and development.

According to [12], multi-risk assessments have been mostly assessed through quantitative tools that aggregate the hazards and vulnerability from a probabilistic perspective. In the frame of the MATRIX project, which aims to set the stages for the multi-risk evaluation for Europe, [13] suggested three tools to address multi-risk assessments: events trees, Bayesian networks and time stepping Monte Carlo simulations. Events trees consider the conditional probability of occurrence of different discrete scenarios of hazards and vulnerabilities, the Bayesian approach analyses the cascade effect of multi-hazard events and time-dependent vulnerability from a probabilistic perspective. Finally, the Monte Carlo approach incorporates the concept of uncertainty in risk evaluation through the generation of multiple random parameters, hazards, and vulnerability scenarios for a given period of time with an associated probability of occurrence. These methodologies require a large and detailed amount of data typically unavailable in many developing countries. Adhering to [14] who stated that multi-risk analyses must acknowledge the vision of stakeholders in the evaluation of all the risk components and the local characteristics of the region under study, this work proposes a simple methodology which fits the needs of regions prone to be affected by multiple natural disasters with insufficient data.

Natural hazards and risk assessment are of extreme relevance for Chile, a country whose average annual economic losses between 1980 and 2011 due to multiple natural disasters have been estimated to represent 1.2% of the gross domestic product, more than for any other country of the G20 group [15]. Moreover, Chile is ranked among the 30 countries under highest water-related risk by 2025, including drought and flood risk [16]. Despite all the territory is highly exposed to multiple natural threats [17], a regulatory framework to support risk management and increase resilience is still under development [11,18,19]. Indeed, the 526 deaths and ~200,000 severely damaged houses caused by the 8.8 Mw Maule earthquake and the subsequent tsunami on 27 February 2010 [20,21], revealed the serious limitations of hazard risk assessments in Chile [22]. Because of these catastrophic losses, and the record of previous hazardous floods and landside episodes in the coastal zone of central Chile [23–25], the Ministry of Housing and Urban Planning (MINVU) and local governments started the development of integrated disaster risk management plans for these areas. These plans must integrate multiple hazards, covering their complex interactions, along with the vulnerability and level of exposure of the community and the infrastructure. Moreover, they must consider the large number of visitors these cities host during the summer season.

This paper presents the development of a multi-risk approach to be applied in urban planning, using two Chilean coastal cities, characterized by low levels of information availability, El Quisco and San Antonio, as a case study. The methods used in the approach are adapted to the local differences of qualitative and quantitative information details. These urban settlements are touristic cities that concentrate a high floating population during summer and are highly exposed to a variety of natural threats that can have large impacts on the local community and economy. This is particularly important, as tourism has experienced continuous growth in the Chilean economy, currently contributing to a 3.3%

of the total domestic gross product (GDP), and the number of foreign visitors has doubled between 2010 and 2016 [26]. A matrix-based multi-risk assessment methodology within the Chilean context is proposed, which integrates the risk associated with different natural hazards including floods, landslide, and tsunami processes. Likewise, as earthquakes act as a triggering factor to tsunamis, the earthquake risk has also been estimated. Despite the lack of detailed data, and the differences in qualitative and quantitative information available for the two cities under analysis, disaster risk is addressed comprehensively considering three different components: the physical characteristics of the hazards, the exposure to single and aggregated hazards, and the physical and socio-economic vulnerability of crucial three elements (i.e., housing, urban infrastructure, and facilities). A mitigation plan orientated to increase the resilience in the cities, using integrated quantitative and qualitative tools to support urban planning in the region is designed and proposed.

2. Materials and Methods

2.1. Study Area

El Quisco and San Antonio are nearby coastal cities located 120 km west of Santiago, the capital of Chile (Figure 1). Both cities have a temperate Mediterranean climate, with a mean annual precipitation of about 500 mm [27]. Because of their proximity to Santiago, these cities are of high touristic interest, especially during summer season, when the population of El Quisco increases up to 8 times [28]. On the other hand, San Antonio is the most important port of the country and the economic hub of the province to which it belongs [29]. The majority of the ~90,000 San Antonio and the ~10,000 El Quisco inhabitants [30] belong to low-income groups identified as highly vulnerable to natural hazards [31,32]. Furthermore, the lack of appropriate regulatory and mitigation plans has led to an unregulated continuous urban development, which has increased the exposure levels to natural hazards.

Figure 1. Location of El Quisco and San Antonio. Rivers and streams are presented in blue lines.

Because its location on the subduction area between the Nazca and the South American plates, several strong tsunamis and earthquakes have occurred in the region [33]. The tsunami of 27 February 2010 [20,34] was particularly destructive and produced severe damages (Figure 2). Furthermore, both cities have developed along the coastal floodplains and near rivers or streams, which enhances the risk to floods and landslide events. Because El Quisco is crossed by five ephemeral creeks (i.e., Las Petras, El Batro, Pinomar, Seminario, and Córdova), there are areas in the city prone to be affected by floods and landslides (Figure 1). On the other hand, San Antonio is crossed by Maipo River and El Sauce stream, and limits to the south with the San Juan stream. According to the [23] report, several fluvial floods and landslide events have affected San Antonio precisely because of the proximity of urban areas to these water bodies.


Figure 2. Damage in the San Antonio area caused by the 27 February 2010 tsunami [35].

2.2. Data and Methodology for Multi-Risk Assessment

Following [1,36] recommendations, a scenario-based multi-risk assessment methodology was developed, which integrates hazard and vulnerability degrees (scores) into a risk matrix, designed to meet the local needs using available local data. Then, MINVU and the local governments provided the information needed to design disaster risk management plans through hazard risk zoning. The methodology schematized in Figure 3 considers the analysis of different degrees of risk for each natural hazard, which are finally overlapped to obtain the multi-risk zoning using Geographic Information System (GIS) tools. First, the natural hazards that have historically affected the study region are identified and characterized, while the exposure to each natural hazard is spatially determined and a level of exposure ranging between 0 (low exposure) to 2.5 (high exposure) is assigned. Based on the standard of recent coastal cities vulnerability studies [37–39], and when qualitative information is available, physical and socio-economical dimensions were considered in the vulnerability assessment of the different components analyzed. Then, a level of vulnerability ranging between 0 (no vulnerability) and 4 (high vulnerability) was assigned to every component evaluated using a matrix. When information about materiality is not suitable to assess the physical vulnerability, only socio-economical dimension is considered, which can be adapted and updated when new information is collated for coastal management plans. Finally, the multi-risk zoning is produced by crossing this matrix and the natural hazard exposure assessment. The range of exposure levels (0 to 2.5), and the vulnerability levels (0 to 4) were defined with the local decision-making authority (i.e., the Chilean Secretary of Regional and Administrative Development, hereafter the SUBDERE), to standardize the level under a 0–10 range. The models and the data used to assess the hazard exposure to the different natural phenomena, the vulnerability and risk characterization are presented in the following sections.
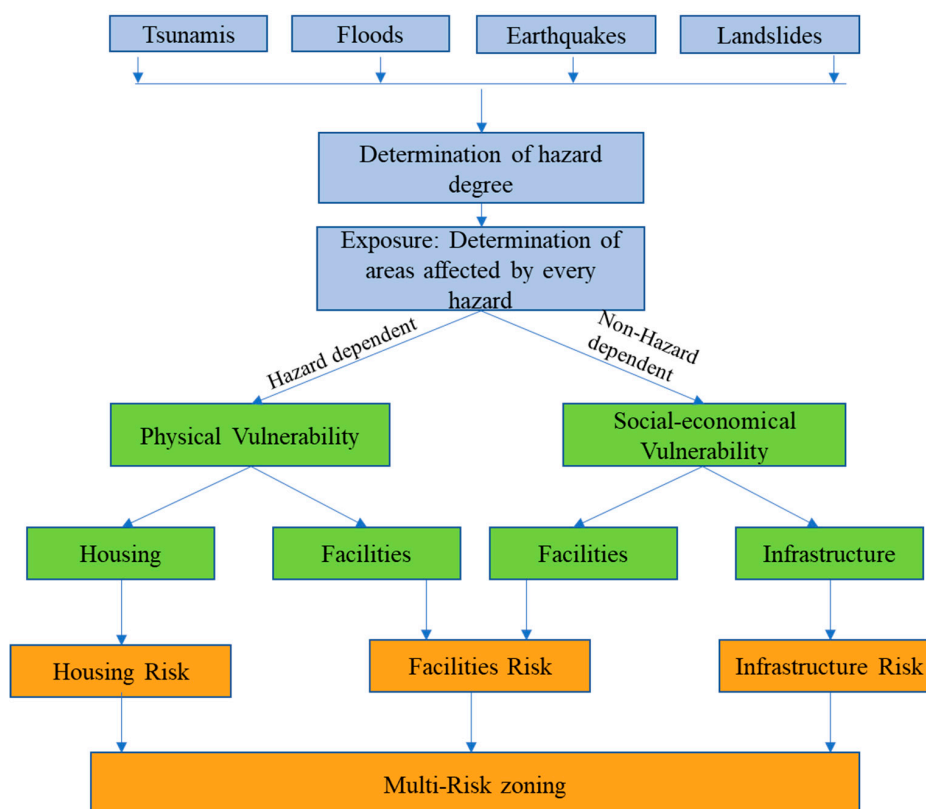
Figure 3. Scheme of the multi-risk assessment methodology. The hazard risk is calculated for each hazard independently, and the overlapping of all the hazards risk determines the multi-risk zoning.

2.2.1. Natural Hazard Characterization

The hazard characterization is developed by constructing scientific physically-based models for each natural phenomenon, extensively used in Chile, to evaluate the exposure to the corresponding hazard (i.e., degree of hazard) considering conservative scenarios and boundary conditions. To standardize the analysis, the degree of hazard is assigned quantitatively using a score or class which was chosen to range from 0 to 2.5, where high (2.5), medium (1–2), and low (0–1.5) degrees of hazard are identified for each natural phenomenon evaluated. Detailed information is provided below.

2.2.2. Flood Hazard

Rainfall-runoff and hydraulic models have commonly been used to characterize the probability of occurrence and the impacts of floods (e.g., [40]). This involves simulating riverine floods associated with precipitation events of different return periods (T), and route them in a hydraulic model. A central assumption then is that T of the flood equals that of the rainfall event that produces it [41]. Based upon the hydraulic design criteria for urban infrastructure specified by the Ministry of Public Works in Chile [23], values of $T = 2, 5, 10, 20, 25, 50$, and 100-year are considered.

Several rainfall-runoff models developed for ungauged basins extensively used in Chile are implemented to simulate the peak flow discharges for different T. These models include (1) the rational method as defined by [41] using the Kirpich formula for computing the time of concentration, (2) the Snyder synthetic unit hydrograph method [42], (3) the Storm Water Management Model (SWMM; [43]); as well as (4) the Verni-King method [44] and (5) the Modified Verni-King Method [45]. These last two models are local methods defined for Chilean catchments, which consider a non-linear relationship between peak flow and contributing area, similar to that of the Espey 10-Min Synthetic Unit Hydrograph [46] and the Colorado Urban Hydrograph Procedure [47]. Parameters for all these models are obtained from the 30 m digital elevation model [48], local studies [35,45,49] and

the literature [41,47]. Local intensity–duration–frequency (IDF) curves and daily precipitation data recorded between 1986 to 2011 at Lagunillas station (33°26′22″ S, 71°27′02″ W) for El Quisco and between 1972–2010 at Punta Panul (33°34′29″ S, 71°37′30″ W) for San Antonio, are utilized to define the rainfall events used in the rainfall-runoff modeling and landslide analysis described later.

The peak flows for the different return periods are propagated using HEC-GeoRAS [50], an ArcGIS® based platform to run the 1D hydraulic model Hec-Ras (Hydrologic Engineering Center River Analysis System; [51]), and display its results. Hec-Ras solves the energy equation (Equation (1)) using an iterative procedure

$$Z_2 + Y_2 + \frac{a_2 V_2^2}{2g} = Z_1 + Y_1 + \frac{a_1 V_1^2}{2g} + h_c \tag{1}$$

where Z is the elevation of the river or channel bed, Y is the water depth, V is the average velocity in the river or the channel, α is the velocity weighting coefficient, and h_c is the energy head loss. Subscript 1 and 2 indicate two sections in the river.

The water surface elevation, the flow velocity and the riverine flooded areas for each stream and return period are obtained from the model. Cross sections measured in the field, contours maps and the 30 m DEM are combined to generate the streambed and floodplain topography, whereas high-tide data from the SHOA (National Hydrographic and Oceanic Service) nautical charts are used to set a conservative downstream boundary condition that maximizes the flooded area (i.e., a water surface elevation of 1.6 m). Finally, the flow discharge record for the period between 1986 and 2011 from the Maipo at Cabimbao gauge (33°43′19″ S, 71°33′18″ W), as well as the topography and other relevant information obtained from local reports [23,29,49,52], are used to calibrate the hydraulic model for the Maipo River.

The level of exposure to flood hazard is categorized based on different scenarios depending on the frequency of the events and following the Organization of American States recommendation [53]. Then, the level of flood hazard exposure was defined as 'low' for a 50-year flood (low frequency), 'medium' for a 20-year flood (medium frequency) in El Quisco (estimated) and 25-year flood in San Antonio (obtained from [23]), and 'high' for a 10-year flood (more frequent).

2.2.3. Landslide Hazard

Landslides are caused by the downward and outward movement of slope-forming materials triggered by the interaction of different conditioning factors. These factors can be the physical characteristics of the terrain (e.g., geomorphology, vegetation, or land use), or external factors such as earthquakes and storms [54], with the last factor being considered in this study. Meteorological variables, particularly precipitation, have the largest impact as a triggering factor of landslides in Chile [55]. The rainfall magnitude and intensity affect the soil moisture before the landslide, increasing the pore pressures and reducing the slope stability. Moreover, precipitation can induce a change in the water table and enhances surface runoff [54].

In this study, landslide hazard is defined by identifying a critical precipitation threshold above which a landslide can occur under a given soil type and topography [56]. This approach allows linking the probability of occurrence of the precipitation event (storm) to the probability of occurrence of the landslide at a specific site. Adapting to the data availability in each city, a physical and a statistical method are used to identify the precipitation threshold in El Quisco and San Antonio respectively. In particular, there was a record of historical landslide events for San Antonio. The physical method used in El Quisco is based on the shallow slope stability (SHALSTAB) model [57], which relates the rainfall rate (P), the pore water pressure (related to W), and the slope stability as

$$W = P \frac{A}{b} T_s sin(\theta) \tag{2}$$

where W (dimensionless) is the wetness, defined as the ratio of the local flux at a given steady state rainfall to that at soil profile saturation. W defines when the saturation overland flow occurs,

which depends on the net rainfall rate (*P*, precipitation less evapotranspiration and deep drainage into bedrock), the contributing area (*A*), the contour length (*b*), the soil transmissivity (*Ts*), and the slope *θ*. The stability in response to a critical precipitation is calculated using the method proposed by [58], which was used to calculate the probability of occurrence of a landslide under different precipitation thresholds.

The statistical method used in San Antonio considers the analysis of the precipitation record and historical landslide events, as suggested by [55]. The method considers the following steps: (1) characterization of historical landslide events by identifying their date, type (debris or mudflow) and triggering factor (precipitation or other factors), (2) analysis of daily precipitation, land use and physical characteristics of the landslide site (conditioning factors), and (3) identification of the magnitude of the triggering precipitation depth and modeling of the conditioning factors that generate the landslides to identify the potentially hazardous areas.

Since the instability of the slope can be the result of either intense precipitation or the saturation of the soil profile because of successive small rainfall events, both the daily rainfall on the day of the event and the cumulative precipitation during the last 20 days are selected as the triggering factors in the statistical method. We also identified the terrain slope and the soil water retention as conditioning factors to landslides. Nineteen different landslide events occurring in San Antonio between 1986 and 2010 are evaluated [23,59,60]. The soil layer depth is obtained from the Chilean Hydrogeologic Map [27], and the land use from the Territorial Master Plan of San Antonio [29].

Both in San Antonio and El Quisco, the level of exposure to landslide hazard is evaluated considering three scenarios based on the return period of the event [61]. Thus, the 50- (less frequent), 20- (medium frequency), and 10- year (more frequent) landslide events are associated with low, medium, and high levels of exposure, respectively.

2.2.4. Tsunami Hazard

Tsunamis represent a threat to coastal cities because the incoming waves have the potential to flood inland areas [62]. A three-step numerical methodology is used to characterize the tsunami hazard, in which (1) the rupture mechanism that originates the tsunami, (2) the regional propagation of the tsunami to the Chilean coast, and (3) the local inundation in the study area, are simulated.

The rupture mechanism was simulated using the Okada model [63], which analytically calculates the surface deformation u_i due to a fault dislocation Δu_j $(\varepsilon_n, \varepsilon_k, \varepsilon_j)$ across a three dimensional surface $\sum (\varepsilon_n, \varepsilon_k$ and ε_j coordinates) produced by shear and tensile faults F (e.g., an earthquake) on an isotropic homogeneous semi-infinite medium

$$u_i = \frac{1}{F} \int_{\Sigma} \Delta u_j \lambda \delta_{jk} \frac{\partial u_i^n}{\partial \varepsilon_n} + \mu \frac{\partial u_i^j}{\partial \varepsilon_k} + \frac{\partial u_i^k}{\partial \varepsilon_j} v_k d \sum \qquad (3)$$

where δ_{jk} is the Kronecker delta, λ and μ are elasticity constants, and v_k is the direction cosine of the normal to the surface element $d \sum$. The parameter values (Table 1) were obtained from a local study developed by [64].

Table 1. Seismic design parameters used in the tsunami modeling, obtained from [65].

Parameter	Tsunami 2010	Scenario 1	Scenario 2
Seismic momentum magnitude (Mw)	8.8	8.6	8.8
Rupture length (km)	550	500	500
Rupture width (km)	100	150	150
Strike	10° N	10° N	10° N
Dip angle	10° to 22°	18°	18°
Slip length (m)	6 to 10	5	10

The regional propagation of the tsunami through the Chilean coast was modeled using the SWAN model (SWAN 41.20AB, Delft University of Technology, Delft, The Netherlands) [66], which solves the non-linear shallow water equations (Equations (4)–(6)) considering Coriolis forces (F_u, F_v), frictional slope effects (Chezy coefficient C) and wind or pressure forces (F_x, F_y)

$$\frac{\partial \eta}{\partial t} + \frac{\partial hu}{\partial x} + \frac{\partial hv}{\partial y} = 0 \tag{4}$$

$$\frac{\partial u}{\partial t} + u\frac{\partial u}{\partial x} + v\frac{\partial u}{\partial y} + g\frac{\partial \eta}{\partial x} = F_v + Fx - g\frac{u\overline{u^2 + v^2}}{C^2 h} \tag{5}$$

$$\frac{\partial v}{\partial t} + u\frac{\partial v}{\partial x} + v\frac{\partial v}{\partial y} + g\frac{\partial \eta}{\partial y} = -F_u + Fy - g\frac{v\overline{u^2 + v^2}}{C^2 h} \tag{6}$$

where η is the vertically averaged flow in terms of horizontal velocity (u,v) and water depth variation (h), and g is the gravity acceleration. The inundation areas at the local level are determined using the nonlinear shallow water model developed by [67] and modified by [68], which propagates rapidly evolving flows over complex topographies using a finite volume approach and a non-orthogonal generalized curvilinear coordinate framework. Topo-bathymetric profiles from the General Bathymetric Chart of the Oceans (GEBCO, http://www.gebco.net), the nautical charts from the SHOA and the study by [65] are used in the regional propagation model.

The regional model for tsunami propagation is coupled with the inundation model by entering the tsunami waves to the local domain using an absorbing-generating boundary condition [69] through a nested grid scheme. To assure numerical convergence, a grid of 0.025° and a time step of 5 s was used in the regional propagation model (i.e., the Courant number is less than 1), and a 30-m resolution grid, restricted by the resolution of the digital elevation model ASTER GDEM (version 2, METI & NASA, USA) [48], is used in the local propagation model. For the whole domain a Manning roughness coefficient of $n = 0.020$ is adopted, representative of smooth natural floodplains [70]. In addition to the information used by the regional propagation model, local topography provided by the cities [29,49] and field data were used in the local inundation model.

We consider inundated areas for one historical and two potential scenarios. The historical scenario used for validation purposes is based on the field measurements taken after the 8.8 Mw Maule earthquake and tsunami [34]. The potential scenarios consider two additional earthquakes of magnitude 8.6 Mw y 8.8 Mw respectively, originated by a rupture located in North-Central Chile, from Santo Domingo to La Serena (33.5° S to 30° S), each with maximum vertical displacements of 1.6 m and 3.2 m, respectively. The regional tsunami model is run in a north–south direction covering ~25° latitude (from Iquique 20° S to Chaitén 45° S), and East-West direction covering 25° longitude of the Chilean coast (~75° W–100° W).

Following [71] recommendations, three scenarios of tsunami degree of hazard are defined: low, medium, and high when the flood depth is less than 0.5 m, between 0.5 and 2 m, and over 2 m respectively.

2.2.5. Earthquake Hazard

Although this work mainly focuses on risks associated with floods, and in order to accomplish the multi-risk assessment for the study area, the earthquake hazard to the extent allowed by the available data and records was also studied. Surface waves from are the main cause of infrastructure damage during large earthquakes. It is well known that the predominant soils and topographic characteristics of an area determine the seismic amplification of these waves [72,73]. As a proxy for seismic amplification, this study considers four soil types (i.e., I, II, III, and IV), where I is a stiff foundation soil, such as rock, characterized by a low seismic amplification, and IV corresponds to a soft deposit, such as soft clays, characterized by a high seismic amplification. Location and information about the soil types in the study area are obtained from [52], while recommendations from Eurocode EN 1998-5:2004 [74] are used to evaluate the topographic

effects on the seismic classification. Hence, topographic effects are neglected when the local slope is lower than 15°, whereas the seismic classification of sectors located within 20 m from areas with slopes ranging between 15° and 30° is increased in one level. Finally, the seismic classification of sectors located near topographic slopes larger than 30° is increased in two levels.

This assessment evaluates the exposure to seismic hazard according to the [53] recommendations, considering three scenarios, which assigns a low, medium, and high degree of hazard to areas with low, medium, and high seismic amplification respectively.

2.3. Vulnerability Characterization

Vulnerability refers to the susceptibility of a community or system of being negatively impacted by a hazard [75,76]. Based upon the results of technical studies developed by the UNESCO-RAPCA (Regional Action Program Central America) project, which since 1999 has been working on the use of GIS and remote sensing tools to assess the impact of natural hazard on human and physical infrastructure in Latin America [77], vulnerability of three components were assessed: housing, facilities (i.e., public and private buildings, equipment, and services) and infrastructure. Table 2 lists the elements considered and evaluated in each component. Depending on the component evaluated, the vulnerability of each element is assessed considering a physical (hazard dependent) and/or a socio-economical (non-hazard dependent) dimension. The physical vulnerability refers to the susceptibility of an element to suffer physical damage because of a hazard. On the other hand, although the socio-economic vulnerability is generally defined as the predisposition of social groups in the context of a natural disaster [78,79], the concept has multiple and complex different definitions [76]. In this study, the socio-economic vulnerability refers to the capacity to respond to a hazard given its relevance and hierarchy in the system [75], which are proxies of the intangible losses of elements at risk in society.

Table 2. Elements at risk.

Housing	Facilities	Infrastructure
Houses	Health services	Roads
Residential buildings	Schools	Bridges
	Police stations	Public lighting
	Naval units	Drinking water infrastructure
	Local government facilities	Telecommunication infrastructure
	Harbors	
	Banks	
	Supermarkets	
	Gas stations	
	Sport centers	
	Government offices	
	Churches	
	Childcare facilities	
	Neighborhood council	
	Other services	

The physical dimension was considered for housing in both study cities, and thus the vulnerability is evaluated in terms of the materials, the quality and the height of the construction [77], whereas for the facilities, the socio-economical vulnerability is evaluated in San Antonio and El Quisco. Nevertheless, as of more detailed information about the building materials and constructions of facilities in El Quisco is available, the physical dimension is also considered in the latter. Finally, the socio-economical dimension is used to evaluate the infrastructure vulnerability in both cities, although the physical vulnerability of roads is also assessed, as information about material and the construction is available. Following the local Chilean Secretary of Regional and Administrative Development criteria (Governmental Office in charge of development of risk plans in Chile), a larger weight to the physical dimension is given through a 3 to 2 proportion. This decision was made

because, under a natural hazard scenario, the physical vulnerability is considered to be more critical than the socio-economical vulnerability when both are estimated for an element. It is worth noting that, although vulnerability definitions normally acknowledge its multi-dimension and site-specific nature [80], most of the scientific studies explore only one of the dimensions of vulnerability of the elements at risk (either the social or physical dimension). Both together, as it is in the case of our study, are rarely considering in the literature [76].

The level of vulnerability is determined based on qualitative parameters following the criteria defined with the Chilean Secretary of Regional and Administrative Development [81] and MINVU, which were then used to be crossed against hazard exposure degrees. To homogenize the evaluation, values of vulnerability level or classes of vulnerability are assigned as 0 (non-vulnerable), 1 (low), 2 (medium-low), 3 (medium-high), or 4 (high) for each element under the physical and the socio-economical dimension separately. Then, the aggregated vulnerability of the elements evaluated under the physical dimension is calculated as the average of the vulnerabilities to the different hazards. The values used to assess the physical vulnerability to every natural hazard are presented in Table 3.

Table 3. Matrix of natural hazards risk scores arisen from the hazard degree and the vulnerability scores.

	Hazard	Tsunami			Fluvial Flood			Landslide			Seismic Wave Amplification		
		High	Medium	Low	High	Medium	Low	High	Medium	Low	High	Medium	Low
Vulnerability	**Score**	**2.5**	**2**	**1.2**	**2.5**	**2**	**0.7**	**2.5**	**1**	**0.4**	**2.5**	**2**	**1.5**
High	4	10	8	4.8	10	8	2.8	10	4	1.6	10	8	6
Medium-High	3	7.5	6	3.6	7.5	6	2.1	7.5	3	1.2	7.5	6	4.5
Medium-Low	2	5	4	2.4	5	4	1.4	5	2	0.8	5	4	3
Low	1	2.5	2	1.2	2.5	2	0.7	2.5	1	0.4	2.5	2	1.5
N/V	0	0	0	0	0	0	0	0	0	0	0	0	0

On the other hand, when the socio-economical dimension is evaluated, single vulnerability values for each element are assigned [82]; these values are not hazard dependent and consider the role of the elements during and after a catastrophic event. The function and characteristics of each element are analyzed, such as the number of students enrolled in each school, the capacity and complexity of health services, among others. For instance, as complex health services have larger capacity to provide medical care during natural disasters than ambulatory health care centers, they are characterized by a larger level of vulnerability. Detailed information about the characteristics considered in the evaluation of each element is presented in Table 4.

Table 4. Vulnerability of facilities, evaluated according to the type of facility and the role they have during and after catastrophic disasters (adapted from [82]).

Health Services	Characteristics-Definition	Socio-Economic Vulnerability
Tertiary health care center	High complexity health service, up to 500 beds	4
Secondary health care center	Medium complexity health service, specialist or referral services	3
Urgency primary health care center	Urgent care center	2
Ambulatory primary health care center	Low complexity health service for ambulatory care	1
Educational Services	**Characteristics-Definition**	**Socio-Economic Vulnerability**
Educational services T1	More than 500 enrolled students	4
Educational services T2	Between 251 and 500 enrolled students	4
Educational services T3	Between 101 and 250 enrolled students	3
Educational services T4	Between 0 and 100 enrolled students	2
Security services	**Characteristics-definition**	**Socio-economic Vulnerability**
Police station T1 ("Comisaría")	High complexity police unit	4
Police station T2 ("Tenencia")	Medium complexity police unit	3
Police station T3 ("Retén")	Low complexity police unit	2
Navy Facilities	**Characteristics-Definition**	**Socio-Economic Vulnerability**
Harbormaster facilities	Ultimate navy regional authority	4
Water bailiff facilities	Local navy authorities controlled by the Harbormaster	3
Navy staff offices	Local navy facilities	2
Local Government Facilities	**Characteristics-Definition**	**Socio-Economic Vulnerability**
Town hall	Local Government administration office	4
Town hall offices	Various governmental agencies controlled by the Town Hall	2

Table 4. *Cont.*

Small harbours facilities-N° of fisherman	Socio-Economic Vulnerability
>200	4
50–200	3
<50	2

Services- Type of facility	Socio-Economic Vulnerability
Bank	2
Supermarket	2
Gas Station	2
Other services	2

Sport Facilities	Characteristics-Definition	Socio-Economic Vulnerability
Stadium	Large capacity sport facility	4
Fitness center	Medium to low capacity sport facility	2
Football court	Medium to low capacity sport facility	2

Other Facilities	Characteristics-Definition	Socio-Economic Vulnerability
Government offices	Provide shelter and help during and after disasters	2
Churches	Provide shelter during and after disasters	2
Child care facilities	Provide shelter and services during and after disasters	2
Neighborhood council	Provide shelter and services during and after disasters	2
Other services	Provide shelter and services during and after disasters	2

Housing vulnerability to tsunami and fluvial floods was assessed following the [77,81] recommendations. Thereby, higher buildings present lower vulnerability than single-story ones. The level of vulnerability to landslides of building is defined as high for all the constructions. Regarding seismic amplification, the assessment considers lower vulnerabilities for lower buildings, as they typically have larger seismic resistance. Table 5 shows the values used to characterize housing vulnerability.

Table 5. Housing level of vulnerability to natural hazards in San Antonio (SA) and El Quisco (EQ) (I: inundation due to tsunami and fluvial flood, LS: landslide, SA: seismic amplification). Note that values may differ for the same hazard among the locations.

Material	I		LS	SA	Condition	I		LS	SA		Height	I	LS	SA
	SA	EQ				SA	EQ		SA	EQ				
Concrete	0	0		0	Good	0	0		1	0	>2 Story	1		4
Bricks	0	1		1	Regular-Good	-	1		-	1	2 Story	2	4	2
Clay	2	2	4	2	Regular	2	2	4	2	2	1 Story	4		1
Wood	3	3		3	Regular Bad	-	3		-	3				
Waste	4	4		4	Bad	4	4		4	4				

Following [81] recommendations to assess infrastructure vulnerability, medium-low and low physical vulnerability are considered for paved roads under different natural hazards, whereas unpaved roads have medium-high physical vulnerability to all the hazards (Table 6). All the infrastructure and facilities elements were considered to have a High physical vulnerability to landslides. Likewise, because road surfaces materials do not provide seismic resistance information, all the infrastructure is evaluated with high physical vulnerability level to this hazard. The socio-economical vulnerability of roads was assessed considering their hierarchy in the city road system, which depends on their size (Table 6).

Table 6. Infrastructure physical and social-economical vulnerability (adapted from [83]).

Road Surface	Physical Vulnerability
Asphalt	1
Gravel	2
Improved dirt	3
Dirt	4
Road Surface	**Physical Vulnerability**
Asphalt	4
Gravel	4
Improved dirt	4
Dirt	4
Type of Road	**Social-Economical Vulnerability**
Paved road	4
Unpaved road	4
Trail	1
Path	1
Type of Road Associated with the Bridge	**Social-Economical Vulnerability**
Paved road	4
Unpaved road	4
Trail	1
Path	1
Lightning Category	**Social-Economical Vulnerability**
Substation	4
Transformer	2
Urban lightning	1
Type of Antenna	**Social-Economical Vulnerability**
Radio antenna	4
Mobile antennas	3
Television antennas	2

Regarding facilities, the socio-economical vulnerability is evaluated for every single element considering its importance or role within the city under a given hazard. Detailed information for each element is presented in Table 4. Finally, the demographic and economic characteristics of the study area are obtained from national and regional studies and entities (i.e., [23,30], the Traffic Headquarters of the Ministry of Public Works, the Communal Planning department and the Education Ministry).

2.4. Risk Characterization

Following the matrix approach, risk is characterized using risk scores calculated as the multiplication of the level of vulnerability and the exposure [6,83] of each evaluated element (i.e., housing, facilities, and infrastructure). Four different risk levels are defined for each hazard in each location: high, medium-high, medium-low, and low, and the scores of these levels are presented in Table 7. Finally, as shown in Figure 3, the integrated multi-risk zoning is defined as the overlapping of the level of risk associated with every hazard, which is presented for each of the elements evaluated separately (i.e., one multi-risk zoning is considered for housing, for facilities, and for infrastructure independently). To be conservative with the results of the risk assessment and following the local decision-making authority (SUBDERE) goal of informing the aggregated risk level (although the hazards do not necessarily have the same probability of occurrence), when overlapping the level of risk associated with each hazard, the highest level of risk predominates for each element.

Table 7. Risk scores for each natural hazard.

Degree of Risk	Risk Score
High	6.1–10
Medium-high	4.1–6
Medium-low	2.1–4
Low	0.1–2
No risk	0
Outside the hazard zones	-

3. Results
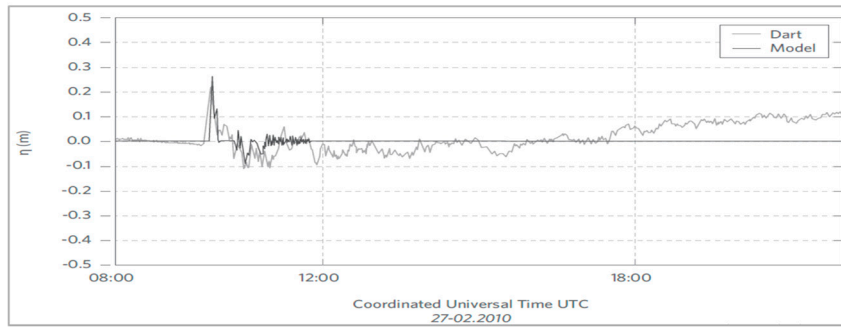
3.1. Natural Hazards

3.1.1. Models Validation

The regional tsunami model is validated by the [65] study using the observations of the 27 February 2010 tsunami. The far-field wave simulated by the SWAN model were compared to the DART (Deep-ocean Assessment and Reporting of Tsunamis) buoy measures located in the coast of Perú (Figure 4a). The near-field waves simulated by the SWAN model were validated by comparing the simulated times of arrival of waves to different Chilean coastal cities against observations published in local media (i.e., La Tercera newspaper, 26 March 2010, Figure 4b).

The fluvial flood model for the Maipo river was validated by comparing the simulated flooded area produced on 8 October 2009 by the flow discharge measured at the Cabimbao station, against a digital photography of the river retrieved from Google Earth (Figure 4c) on the same day. Also, other historical floods reported by [23] are used to validate the models for other streams. On the other hand, the SHALSTAB landslide model is validated in San Antonio through its ability to simulate the location of a landslide event in the 'Talud 21 de Mayo' sector that took place on 28 May 2013, which was produced by a 5- to 10-year rainfall event (Figure 4d).
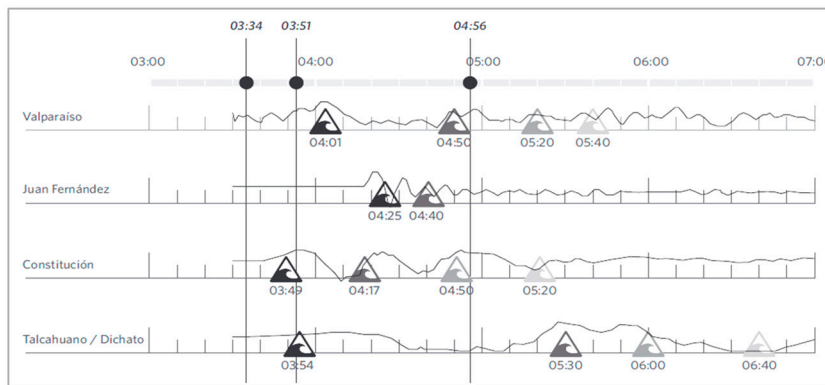
Finally, the seismic wave amplification classification could not be quantitatively validated due to the lack of proper instrumentation in the zone. Nonetheless, because the soil type II representative of a low level of amplification is predominant in both cities under study, significant uncertainty in the risk assessment is not expected.
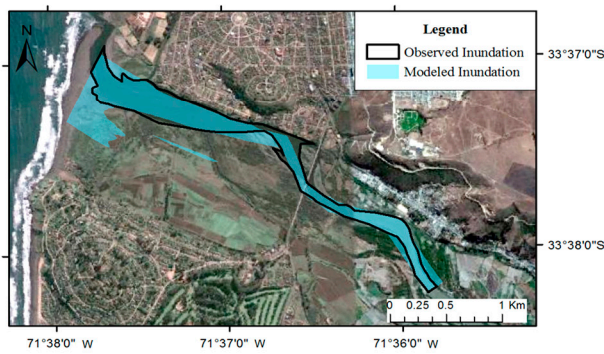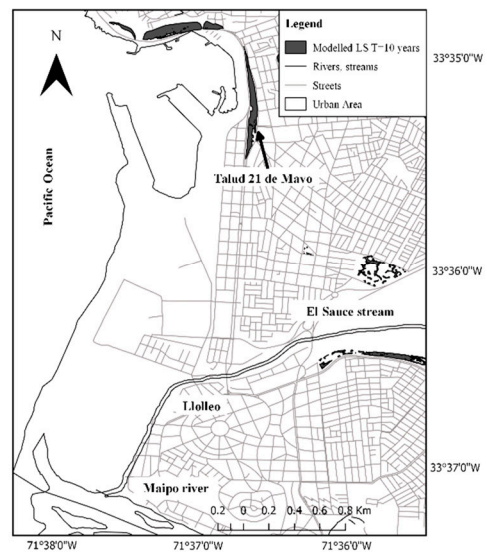
a)

b)

c)　　　　　　　　　　　　　　　　　　　　d)

Figure 4. Validation of natural hazard models. (**a**) Validation of the SWAN model by comparing the far-field wave simulation to the DART buoy measures located in the coast of Perú. (**b**) Validation of the near-field SWAN model waves by comparing simulated times of arrival to different Chilean coastal cities against observations published in local media. (**c**) Validation of the flood inundation model using the flooded area retrieved from Google Earth V 6.2 for 8 October 2009. (**d**) Validation of the landslide model through the simulation of the landslide occurred on 28 May 2013 in Talud 21 de Mayo zone under the 5- to 10-year precipitation event.

3.1.2. Natural Hazards Model Results

Results of the regional tsunami propagation model toward the coastline of El Quisco and San Antonio indicate that, for the 8.6 Mw scenario, the first tsunami wave has a maximum amplitude of 1.5 m and reaches the coastline within the first hour of simulation. Simulations under the 8.8 Mw scenarios indicate that the first tsunami wave has a maximum amplitude of 4 m arriving to the Chilean coast within 30 min after the rupture. According to the simulations, inundation extents obtained from the local propagation model over El Quisco are relatively small under both the 8.8 Mw and 8.6 Mw scenarios. Only the beaches, the mouth of streams and some coastal streets are flooded in the model, with inundation depths of ~2 m and ~0.5 m under the 8.8 Mw and 8.6 Mw scenarios respectively (Figure 5a). On the other hand, larger inundations areas are obtained in San Antonio. The harbor, downtown, and some residential sectors located along the streams and the Maipo river are flooded due to the tsunami propagation upstream. As expected, a larger inundation extent is obtained under the 8.8 Mw scenario. The maximum water depths under the 8.8 Mw and 8.6 Mw scenarios are 5 m and 4 m respectively along the coast of San Antonio (Figure 5b).
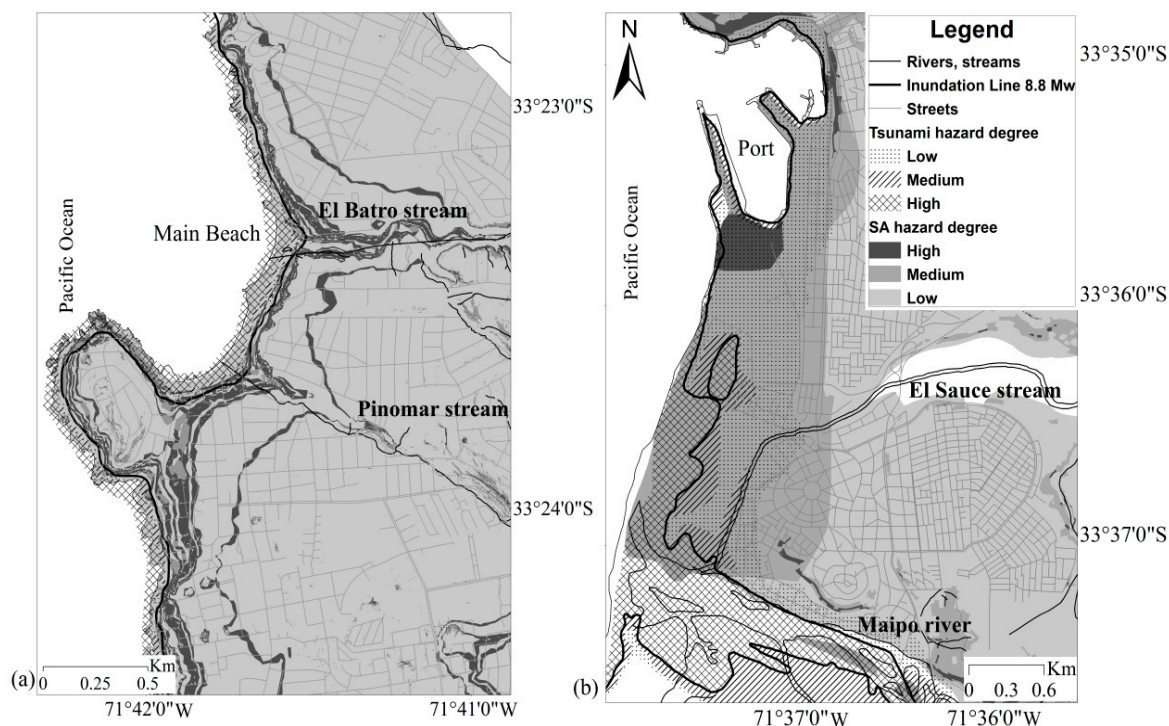
Figure 5. Integrated degree of hazard due to seismic wave amplification (SA) and tsunami inundation at (**a**) El Quisco and (**b**) San Antonio.

Regarding the fluvial flood modeling, simulated inundation areas due to fluvial floods are larger for San Antonio than for El Quisco (Figure 6a,b). Large flooded areas are simulated in the urban sectors bordering the streams and the Maipo river. Maximum velocities of ~5 m/s are reached under the 100-year flood. Urban areas adjacent to El Sauce stream and the Maipo river become flooded with the 2-year flood and the 10-year flood respectively, whereas considerable large flooded areas are obtained for events larger than the 25-year flood. Furthermore, inundations are simulated for flood events with a recurrence interval of 2-years or larger near the San Juan stream and in the crops yields located between this stream and the Maipo River. On the other hand, simulations at El Quisco show that the streams banks start overflowing in some urban sectors for events larger than the 2-year flood. Floods are simulated at the Cordova stream for events larger than the 5-year flood.
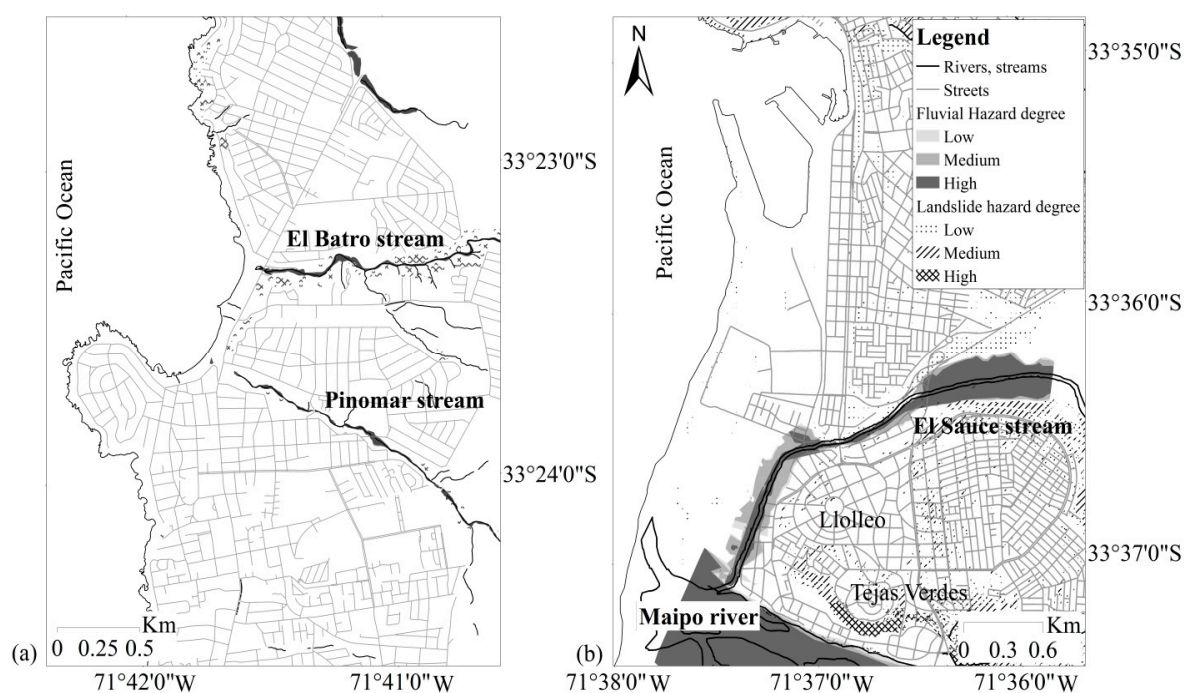
Figure 6. Integrated degree of hazard due to fluvial flood inundations and landslides triggered by 10-, 20-, 25-, and 50-year rainfall at (**a**) El Quisco and (**b**) San Antonio.

San Antonio is more likely to be affected by landslides than El Quisco (Figure 6a,b). Landslide events are prone to occur only in the north part of the main beach of El Quisco, which are expected to be initiated by a 5-year rainfall critical threshold. In the case of San Antonio, the simulations indicate that Llolleo, the Tejas Verdes sectors and the road to San Juan, all located in the southern part of the city, are prone to landslides triggered by a 5-year rainfall threshold. On the other hand, in downtown area landslide events can be initiated by a 50-year rainfall event.

Finally, the analysis of the seismic wave amplification shows that a large part of El Quisco is founded on soils type II which are associated with a low hazard degree, while San Antonio is majorly founded on soils type II and III (i.e., medium degree of hazard), and soils type IV (high degree of hazard) in some locations. Sectors with steep slopes in both cities are prone to be affected by topographic amplification, which increases the hazard degree (Figure 5a,b).

3.2. Vulnerability Evaluation

The housing elements at El Quisco and San Antonio have similar vulnerability to natural hazards (Figure 7a,b). According to the results, housing at El Quisco predominately has a medium-high vulnerability (65%) and medium-low (30%) vulnerability to tsunami and flood inundations respectively. Furthermore, housing in El Quisco has High vulnerability (95%) to landslides and low and medium-Low (50% and 48%, respectively) vulnerability to seismic amplification. The vulnerability of facilities at El Quisco ranges from Low to High considering different elements and hazards. Mostly medium-high to high vulnerability to landslides and medium-low and low vulnerability to seismic amplification is observed. Most vulnerable facilities are those related to health and the educational services, which are crucial as they provide support and shelter in the aftermath of natural disasters. In El Quisco these elements are located in areas prone to fluvial inundations.
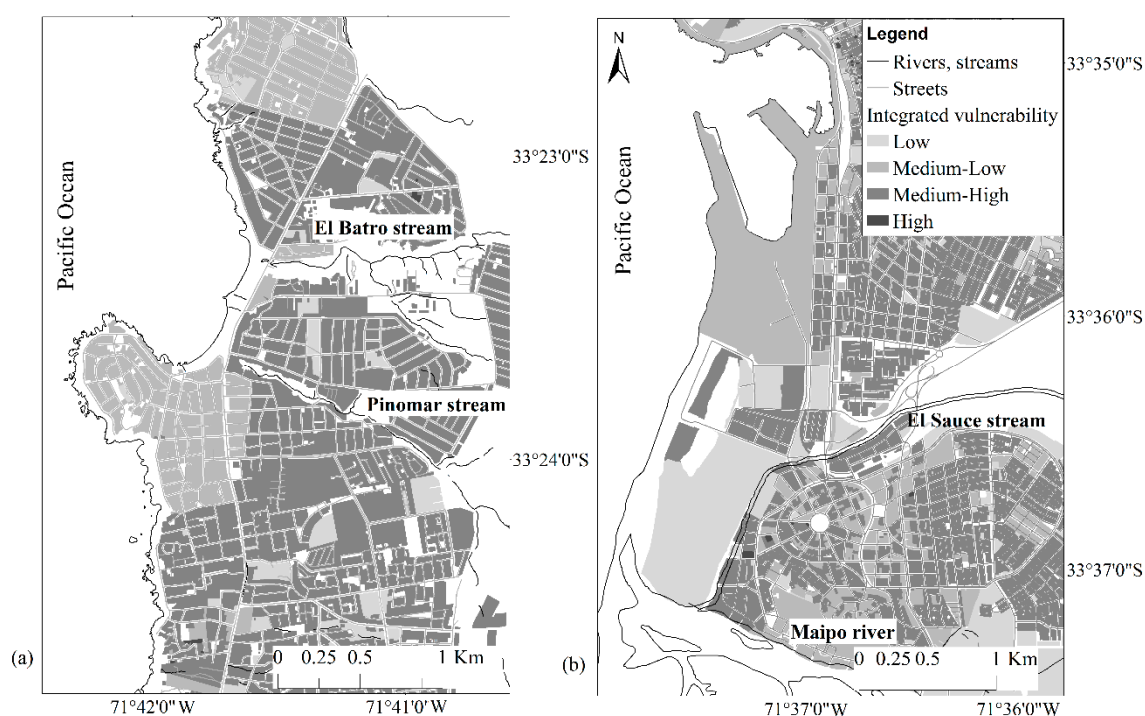
Figure 7. Integrated vulnerability of housing in (**a**) El Quisco and (**b**) San Antonio.

The evaluation of housing at San Antonio indicates that the city presents mostly medium-low (46%) and medium-high (28%) vulnerability to tsunami and flood inundations, high (94%) vulnerability to landslides processes and low and medium-low (62% and 33%, respectively) vulnerability to seismic amplification. Likewise, depending on the evaluated element, facilities have vulnerabilities ranging between high to low.

The vulnerability in both cities ranges from low to medium-high for electricity and telecommunication infrastructure, and from medium-high to high for water supply systems. Major differences are observed for road networks, as El Quisco has mostly unpaved roads and the vulnerability to inundations and to landslides ranges from high to medium-high. On the other hand, roads at San Antonio have a low vulnerability to tsunami and fluvial inundations.

3.3. Risk Evaluation

As indicated in Section 2.2.3, although is very unlikely that the four hazards here considered have the same probability of occurrence, with the purpose of informing and designing conservative mitigation plans, the local authority SUBDERE recommends aggregating the levels of risk of all the natural hazards. Despite that, the levels of risk of every hazard in an independently manner was also assessed (not showed).

Overall, San Antonio is more at risk to natural hazards than El Quisco when considering housing and facilities, but both cities have a similar risk with respect to infrastructure elements. Because of the low exposure of houses at El Quisco, they have a low risk to tsunami and flood inundations and landslides processes. Regarding facilities, only little harbors have a medium-high risk to inundations (Figure 8a). Furthermore, housing and facilities risk to seismic amplification waves range between low to medium-low and between medium-low to medium-high, respectively.

Housing risk to tsunamis at San Antonio ranges between medium-low to medium-high. In particular, a high risk is identified in the Llolleo lagoon sector (North of the Maipo estuary, Figure 8b), where the inundation depth exceeds 2.5 m and houses are highly vulnerable to the threat. The San Antonio housing sector has all the levels of risk to fluvial floods depending on the location. Because of the high vulnerability and the high degree of hazard to inundation of the sectors bordering the streams in San Antonio, they have high level of risk. On the other hand, the housing sector is at medium-low

to low risk to landslides, except for the Tejas Verdes and San Juan locations, where a high risk is identified due to their High exposure to the hazard. Regarding facilities, a medium-high risk to tsunami is observed in the city, and only around the Llolleo area a high risk to fluvial flood is detected. A high, medium-low, and low risk to landslide events is identified for the facility sector, whereas a medium-low, medium-high, and high risk to seismic amplification is detected in different zones of the city. Finally, no risk to inundations or landslides is detected for the infrastructure in both cities, as there is no exposure. On the contrary, almost all the infrastructure sector is at high risk to seismic amplification in both cities.
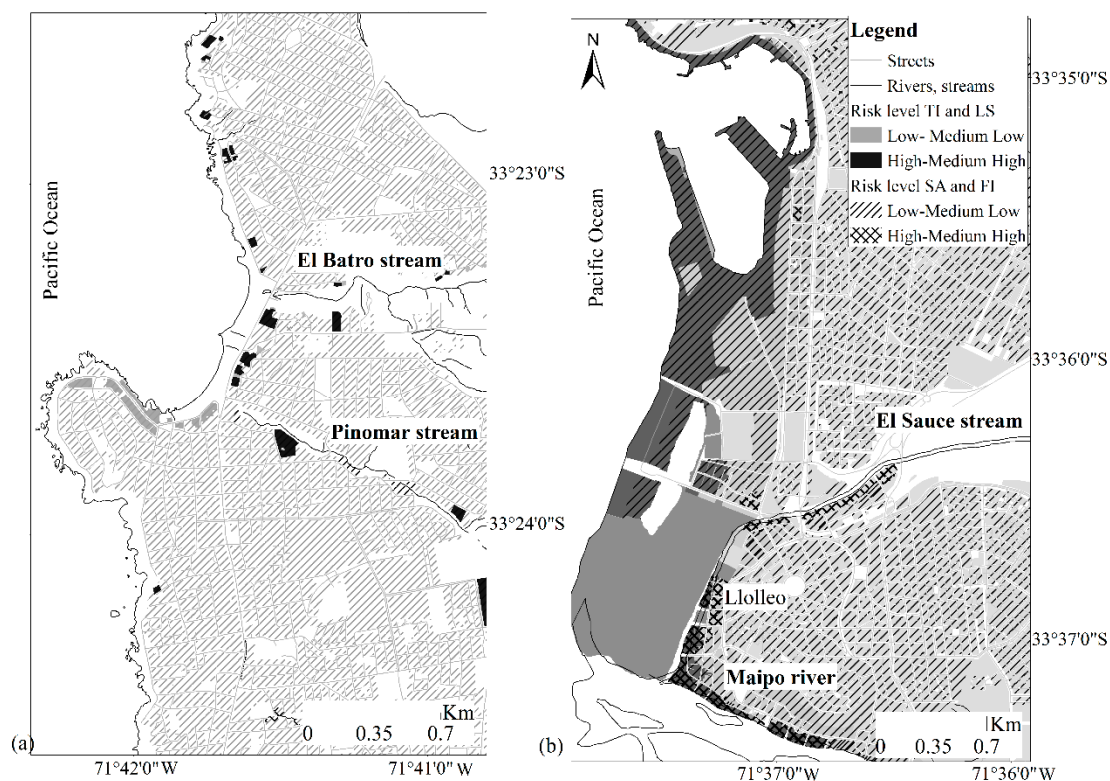
Figure 8. Housing integrated level of risk in (**a**) El Quisco and (**b**) San Antonio. The figures consider the Tsunami inundation (TI), landslide (LS), seismic amplification (SA), and fluvial inundation (FI) risk levels.

3.4. Multi-Risk Analysis

The threats analyzed in this study can potentially occur simultaneously, increasing the risk to natural hazards in the region. For instance, a large earthquake in the coastal sector can trigger a tsunami, or a strong rainfall event might cause floods and landslides simultaneously. The results for exposure to seismic amplification and tsunami hazards are presented in Figure 5a,b. El Quisco has a low degree of exposure to tsunami and seismic wave amplification, excepting some regions like the coastal line (Figure 5a). Figure 5b shows that the port and the coastline of San Antonio is highly exposed to these natural hazards. Despite half of the population is in areas with a low degree of exposure to these hazards, large urban sectors are located in areas with a medium degree of exposure to the combined effect of tsunami and seismic wave amplification. On the other hand, the aggregated analysis of landslides and fluvial flood hazards is presented in Figure 6. High exposure to fluvial flood and landslide is identified along the streams at El Quisco; however, no urban areas are involved (Figure 6a). On the contrary, significant urban areas are affected by one of the two natural hazards in San Antonio (Figure 6b); the sector bordering the Maipo river and streams are highly exposed to landslide and fluvial flood hazards.

Regarding a crossed vulnerability analysis, both cities have a medium-high housing (Figure 7) and facility vulnerability. The assessment of the multi-hazard risk for housing (Figure 8) indicates that risk is mainly low and medium-low in both cities. A larger risk is detected in some sectors of San Antonio, because of the large exposure to floods and landslide previously discussed. Despite the high facility vulnerability, facilities in El Quisco are at low risk, as they are not exposed to floods or landslides (Figure S1, Supplementary Material). Conversely, the facilities in San Antonio are at high risk because of their high exposure to these hazards. Out of the possible risks, the seismic wave amplification risk is the highest in both cities due to the high vulnerability to this hazard.

Overall, El Quisco is better prepared than San Antonio to deal with natural hazards (Figure 8). However, some of the low risk areas correspond to uninhabited places such as location 1 in Figure S2 (Supplementary Material), where future urban development might increase the risk to natural hazards. Finally, note that the risk analysis is carried out at a block (i.e., polygon) scale, while the exposure to the hazard is calculated at the grid-cell level. Thus, every block is given the highest risk computed for each of the grid-cells belonging to that block.

3.5. Mitigation and Evacuation Plans

The results of the multi-risk assessment show that integrated risk management plans to reduce life and properties losses and to increase resilience, are to be undertaken urgently in the study area. Although the risk zoning presented in this paper can be used to design and evaluate engineering measures to alleviate the risk, this is out of the scope of this research, which mostly focuses on characterizing the current risk state. This characterization provides the basis for the subsequent planning and assessment of mitigation measures. Recommendations from the literature [62,84] are adapted to the local conditions to design a risk mitigation plan, which considers the following main guidance:

- Relocation of the population living nearby the Llolleo lagoons (estuary of Maipo river) in San Antonio. Such action will enhance the development of dune systems, creating a buffer zone against tsunamis.
- Local and regional impact assessment and definition of mitigation infrastructure in case that any expansion of the San Antonio port is planned. Furthermore, a safe location of the stacking areas must be ensured, along with a contingency plan to control the damage caused by ships that can be dragged during tsunamis events.
- Restriction to new developments near streams and the Maipo River. In addition, mitigation infrastructure should be considered to protect existing constructions in the area. Special attention should be drawn to south Llolleo, which is highly exposed to landslides events.
- More control over the extraction of aggregates from the Cordova stream in El Quisco to reduce flood and tsunami risks.

In addition to these measures, the development of evacuation plans for both cities to cope with tsunamis becomes essential [85]. Using the risk zoning previously identified along with the topography and the existent road infrastructure, we identify evacuation routes and characterize traveling times to safe zones for both cities (Figure 9). For this purpose, four steps are considered:

1. Construction and updating of the information of road axes, including the road impedance and traveling times in each road.
2. Definition of safe areas and evacuation times under the worst modeled scenario (i.e., an 8.8 Mw earthquake and tsunami with critical evacuation times of 10, 15, and 60 min [86].
3. Definition of evacuation roads based on the urban layout, the relief and the safe zones in the city, which were located in open and flat areas able to receive a large number of people [87].
4. Identification of evacuation roads with slopes lower than 12%, in which stairs must be avoided. Areas with evacuation times over 15 min must be considered as uninhabitable zones in the urban design of the cities.

Overall, El Quisco is better prepared than San Antonio for an evacuation due to Tsunami, as the majority of the most distant locations to the safe zone are not residential (Figure 9). Nevertheless, alternative routes to the main roads and clear signals indicating the evacuation roads must be considered for El Quisco in order to facilitate the possible evacuation of summer floating population.
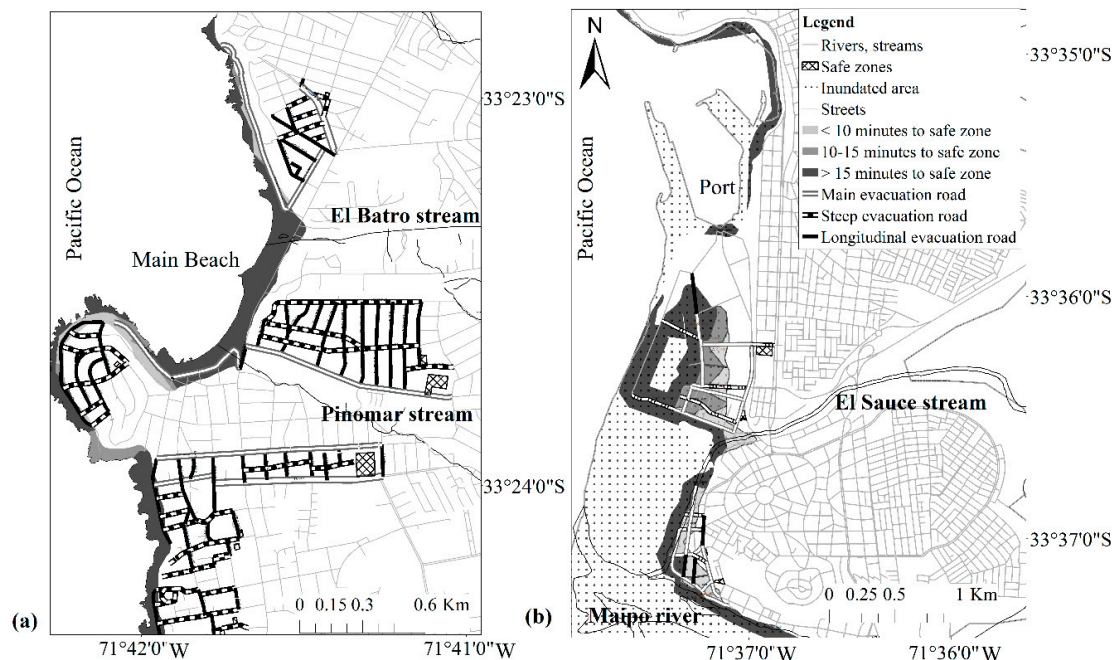

Figure 9. Tsunami evacuation plan at (**a**) El Quisco and (**b**) San Antonio.

4. Conclusions

This study successfully performs a simplified multi-risk evaluation of areas prone to be affected by natural hazard in El Quisco and San Antonio, two coastal cities in Central Chile. The natural hazards considered include tsunamis, fluvial floods, landslides, and seismic amplification, with the aim of supporting urban planning instruments and mitigation plans to increase resilience. Using simple calculations based on available data, a cross-analysis of multiple hazards and the multi-vulnerability estimation of housing, facilities, and infrastructure from a physical and socio-economical perspective was conducted. Adhering to [1,14], a matrix-based multi-risk methodology was designed that considers the local needs incorporated through the experience and opinion of the regional stakeholders. Such approach increases local level engagement in building and implementing disaster risk reduction and resilience thinking plans. Finally, mitigation measures for both cities were recommended based on the results of the assessment. Although the methodology implemented in this study was based on local-level data and stakeholder appreciation, we hope the results can be extended to other coastal cities and regions in Chile and other areas prone to be affected by the hazards here considered. The main conclusions of the study are:

1. Despite the short distance between the cities and similar vulnerability to the evaluated natural hazards, their local characteristics produce very different levels of risk. This highlights the importance of local characteristics when assessing the risk and developing suitable mitigation plans.
2. Disaster risk management plans should consider multi-risk methodologies instead of a single hazard approach. The multi-risk approach demonstrates that exposure to hazards and the risk increase when multiple hazards are considered.
3. Evacuation plans for tsunamis are particularly important for these cities. Plans should consider clear and safe routes that can be used during summer, when floating population increases the vulnerability to natural disaster. Another relevant aspect is the development of urban planning tools that restrict future urban development near streams to reduce flood and landslide risks.

The lack of extensive and detailed data is an important shortcoming when implementing physically based hazard models. Thus, future assessments should consider a probabilistic approach such as the FEMA P-58 frame [88] to account for uncertainties in the calculations and improve the characterization and evaluation of hazards and vulnerability. Furthermore, seismic instrumentation, detailed soil characterization, and bathymetric profiles of streams and the shore should also be incorporated. On the other hand, if the qualitative information used to characterize the vulnerability is improved, the methodology here presented should be updated to consider both the physical and the socio-economical dimensions of vulnerability for every component under assessment.

Despite risk management in Chilean coastal cities is critical, the country lacks a methodology and criteria to assess and manage risk. Next stages in Chilean risk management should focus on (1) the consolidation of a methodology like the one presented here, which considers a probabilistic and cascade effect of the multi-hazard and multi-vulnerability; and on (2) the implementation of risk mitigation plans oriented to exposure and vulnerability reduction, to be prepared for the next disaster. These plans should be constantly evaluated and updated as new natural disasters take place and new data are available.

References

1. Field, C.B.; Barros, V.; Stocker, T.F.; Dahe, Q. *Managing the Risks of Extreme Events and Disasters to Advance Climate Change Adaptation: Special Report of the Intergovernmental Panel on Climate Change*; Cambridge University Press: Cambridge, UK, 2012.

2. Neumann, B.; Vafeidis, A.T.; Zimmermann, J.; Nicholls, R.J. Future Coastal Population Growth and Exposure to Sea-Level Rise and Coastal Flooding-a Global Assessment. *PLoS ONE* **2015**, *10*, e0118571. [CrossRef] [PubMed]

3. Stocker, T.F.; Qin, D.; Plattner, G.-K.; Tignor, M.; Allen, S.K.; Boschung, J.; Nauels, A.; Xia, Y.; Bex, V.; Midgley, P.M. *Climate Change 2013: The Physical Science Basis. Contribution of Working Group I to the Fifth Assessment Report of the Intergovernmental Panel on Climate Change (AR5)*; Cambridge Univ Press: New York, NY, USA, 2013.

4. Álvarez, G.; Quiroz, M.; León, J.; Cienfuegos, R. Identification and Classification of Urban Micro-Vulnerabilities in Tsunami Evacuation Routes for the City of Iquique, Chile. *Nat. Hazards Earth Syst. Sci.* **2018**, *18*, 2027–2039. [CrossRef]

5. Crichton, D. The Risk Triangle. In *Natural Disaster Management*; Tudor Rose: London, UK, 1999; pp. 102–103.

6. ISDR. *Living with Risk: A Global Review of Disaster Reduction Initiatives*; United Nations Publications, International Strategy for Disaster Reduction: Geneva, Switzerland, 2004; Volume 1.

7. UNISDR. *Terminology: Basic Terms of Disaster Risk Reduction*; UNISDR: Santiago, Chile, 2009.

8. Camarasa-Belmonte, A.M.; Soriano-García, J. Flood Risk Assessment and Mapping in Peri-Urban Mediterranean Environments Using Hydrogeomorphology. Application to Ephemeral Streams in the Valencia Region (Eastern Spain). *Landsc. Urban Plan.* **2012**, *104*, 189–200. [CrossRef]

9. Sepúlveda, S.A.; Rebolledo, S.; McPhee, J.; Lara, M.; Cartes, M.; Rubio, E.; Silva, D.; Correia, N.; Vásquez, J.P. Catastrophic, Rainfall-Induced Debris Flows in Andean Villages of Tarapacá, Atacama Desert, Northern Chile. *Landslides* **2014**, *11*, 481–491. [CrossRef]

10. Chen, H.X.; Zhang, S.; Peng, M.; Zhang, L.M. A Physically-Based Multi-Hazard Risk Assessment Platform for Regional Rainfall-Induced Slope Failures and Debris Flows. *Eng. Geol.* **2016**, *203*, 15–29. [CrossRef]

11. Villagra, P.; Herrmann, G.; Quintana, C.; Sepúlveda, R.D. Resilience Thinking and Urban Planning in a Coastal Environment at Risks of Tsunamis: The Case Study of Mehuín, Chile. *Rev. Geogr. Norte Gd.* **2016**, *82*, 63–82. [CrossRef]

12. Gallina, V.; Torresan, S.; Critto, A.; Sperotto, A.; Glade, T.; Marcomini, A. A Review of Multi-Risk Methodologies for Natural Hazards: Consequences and Challenges for a Climate Change Impact Assessment. *J. Environ. Manag.* **2016**, *168*, 123–132. [CrossRef] [PubMed]

13. Fleming, K.M.; Zschau, J.; Gasparini, P.; Modaressi, H.; Consortium, M. New Multi-Hazard and MulTi-RIsk Assessment MethodS for Europe (MATRIX): A Research Program towards Mitigating Multiple Hazards and Risks in Europe. In *AGU Fall Meeting Abstracts*; American Geophysical Union: San Francisco, CA, USA, 2011.

14. Carpignano, A.; Golia, E.; Di Mauro, C.; Bouchon, S.; Nordvik, J. A Methodological Approach for the Definition of Multi-risk Maps at Regional Level: First Application. *J. Risk Res.* **2009**, *12*, 513–534. [CrossRef]

15. CNID-CREDEN. *Hacia Un Chile Resiliente Frente a Desastres: Una Oportunidad*; CNID-CREDEN: Santiago, Chile, 2016.

16. Fundacion Chile. *Desafíos Del Agua Para La Región Latinoamericana*; Fundacion Chile: Santiago, Chile, 2017.

17. Camus, P.; Arenas, F.; Lagos, M.; Romero, A. Visión Histórica de La Respuesta a Las Amenazas Naturales En Chile y Oportunidades de Gestión Del Riesgo de Desastre. *Rev. Geogr. Norte Gd.* **2016**, *64*, 9–20. [CrossRef]

18. UNISDR AM. *Diagnóstico de La Situación de La Reducción Del Riesgo de Desastres Naturales En Chile*; UNISDR AM: Geneva, Switzerland, 2010.

19. ONEMI. *Política Nacional Para La Gestión de Riesgo de Desastres*; ONEMI: Santiago, Chile, 2014.

20. USGS. *Magnitude 8.8 – Offshore Maule, Chile, February 27, 2010*; USGS: Reston, VA, USA, 2010.

21. Ministerio del Interior. *Balance de Reconstrucción*; Ministerio del Interior: Santiago, Chile, 2011.

22. Fariña, L.M.; Opaso, C.; Vera-Puz, P. *Impactos Ambientales Del Terremoto y Tsunami En Chile. Las Réplicas Ocultas Del F, 27. Fund*; TERRAM: Santiago, Chile, 2012.

23. DOH. *Plan Maestro de Evacuación y Drenaje de Aguas Lluvias, San Antonio y Cartagena, V Región*; DOH: Santiago, Chile, 2003.

24. Sepúlveda, S.A.; Rebolledo, S.; Vargas, G. Recent Catastrophic Debris Flows in Chile: Geological Hazard, Climatic Relationships and Human Response. *Quat. Int.* **2006**, *158*, 83–95. [CrossRef]

25. Petley, D. Global Patterns of Loss of Life from Landslides. *Geology* **2012**, *40*, 927–930. [CrossRef]

26. MOP. *Plan Especial de Infraestructura MOP de Apoyo Al Turismo Sustentable a 2030*; MOP: Santiago, Chile, 2017.

27. DGA. *Balance Hídrico de Chile*; DGA: Santiago, Chile, 1987.

28. Gobernación Provincial de San Antonio. *Plan de Seguridad Provincia de San Antonio*; Gobernación Provincial de San Antonio: San Antonio, Chile, 2010.

29. IMSA. *Plan Regulador Comuna de San Antonio*; IMSA: San Antonio, Chile, 2006.

30. INE. *Censo de Población y Vivienda 2002*; INE: Santiago, Chile, 2002.

31. Butz, W.P.; Lutz, W.; Sendzimir, J. Education and Differential Vulnerability to Natural Disasters. *Ecol. Soc.* **2014**.

32. Muttarak, R.; Lutz, W. Is Education a Key to Reducing Vulnerability to Natural Disasters and Hence Unavoidable Climate Change? *Ecol. Soc.* **2014**, *19*, 42. [CrossRef]

33. Lagos López, M. *Tsunamis de Origen Cercano a Las Costas de Chile*; Pontificia Universidad Católica de Chile: Santiago, Chile, 2000.

34. Fritz, H.M.; Petroff, C.M.; Catalán, P.A.; Cienfuegos, R.; Winckler, P.; Kalligeris, N.; Weiss, R.; Barrientos, S.E.; Meneses, G.; Valderas-Bermejo, C. Field Survey of the 27 February 2010 Chile Tsunami. *Pure Appl. Geophys.* **2011**, *168*, 1989–2010. [CrossRef]

35. IMSA. *Efectos de La Ola Sísmica o Tsunami En La Laguna Llolleo*; IMSA: San Antonio, Chile, 2010.

36. Habersack, H.; Schober, B.; Hauer, C. Floodplain Evaluation Matrix (FEM): An Interdisciplinary Method for Evaluating River Floodplains in the Context of Integrated Flood Risk Management. *Nat. Hazards* **2015**, *75*, 5–32. [CrossRef]

37. Kantamaneni, K.; Gallagher, A.; Du, X. Assessing and Mapping Regional Coastal Vulnerability for Port Environments and Coastal Cities. *J. Coast. Conserv.* **2018**, *23*, 59–70. [CrossRef]

38. Fitton, J.M.; Hansom, J.D.; Rennie, A.F. A National Coastal Erosion Susceptibility Model for Scotland. *Ocean Coast. Manag.* **2016**, *132*, 80–89. [CrossRef]

39. Fitton, J.M.; Hansom, J.D.; Rennie, A.F. A Method for Modelling Coastal Erosion Risk: The Example of Scotland. *Nat. Hazards* **2018**, *91*, 931–961. [CrossRef]

40. Kourgialas, N.N.; Karatzas, G.P. A Hydro-Sedimentary Modeling System for Flash Flood Propagation and Hazard Estimation under Different Agricultural Practices. *Nat. Hazards Earth Syst. Sci.* **2014**, *14*, 625–634. [CrossRef]

41. Te Chow, V.; Maidment, D.R.; Mays, L.W. *Hidrología Aplicada*; McGraw-Hill: New York, NY, USA, 1994.

42. Snyder, F.F. Synthetic Unit-graphs. *Eos Trans. Am. Geophys. Union* **1938**, *19*, 447–454. [CrossRef]

43. Rossman, L.A.; Huber, W. *Storm Water Management Model Reference Manual Volume I—Hydrology (Revised)*; US Environ. Prot. Agency: Cincinnati, OH, USA, 2016.

44. Verni, F.; King Farias, H. *Estimación de Crecidas En Cuencas No Controladas*; Sociedad Chilena Ingenieria Hidraulica: Santiago, Chile, 1977; pp. 357–374.

45. DGA. *Manual de Cálculo de Crecidas y Caudales Mínimos En Cuencas Sin Información Fluviométrica*; DGA: Santiago, Chile, 1995.

46. Espey, W.; Altman, D.G.; Graves, C. *Nomographs for Ten-Minute Unit Hydrographs for Small Urban Watersheds*; Issue 32 of Technical Memorandum; American Society of Civil Engineers Urban Water Resources Council: Reston, VA, USA, 1977.

47. Viessman, W.; Lewis, G.L. *Introduction to Hydrology*, 5th ed.; Prentice Hall/Pearson Education: Upper Saddle River, NJ, USA, 2003.

48. NASA. *ASTER Global Digital Elevation Model [Data Set]*; NASA: Washington, DC, USA, 2009.

49. IMEQ. *Plan Municipal de Cultura Comuna de El Quisco 2014–2016*; IMEQ: El Quisco, Chile, 2014.

50. USACE. *HEC-GeoRAS GIS Tools for Support of HEC-RAS Using ArcGIS© User's Manual Version 4.3*; USACE: Washington, DC, USA, 2011.

51. USACE. *HEC RAS, River Analysis System User's Manual, v. 4.0*; USACE: Washington, DC, USA, 2008.

52. CIREN. *Estudio Agrológico V Región*; CIREN: Santiago, Chile, 1997.

53. OAS. *Primer on Natural Hazard Management in Integrated Regional Development Planning*; Organization of American States, Department of Regional Development and Environment ExecutiveSecretariat for Economic and Social Affairs: Washington, DC, USA, 1991.

54. Highland, L.; Bobrowsky, P.T. *The Landslide Handbook: A Guide to Understanding Landslides*; US Geological Survey Reston: Reston, VA, USA, 2008.

55. Sepúlveda, S.A.; Padilla, C. Rain-Induced Debris and Mudflow Triggering Factors Assessment in the Santiago Cordilleran Foothills, Central Chile. *Nat. Hazards* **2008**, *47*, 201–215. [CrossRef]

56. Guzzetti, F.; Peruccacci, S.; Rossi, M.; Stark, C.P. The Rainfall Intensity—Duration Control of Shallow Landslides and Debris Flows: An Update. *Landslides* **2008**, *5*, 3–17. [CrossRef]

57. Montgomery, D.R.; Dietrich, W.E. A Physically Based Model for the Topographic Control on Shallow Landsliding. *Water Resour. Res.* **1994**, *30*, 1153–1171. [CrossRef]

58. Guimaraes, R.F.; Montgomery, D.R.; Greenberg, H.M.; Fernandes, N.F.; Gomes, R.A.T.; de Carvalho Júnior, O.A. Parameterization of Soil Properties for a Model of Topographic Controls on Shallow Landsliding: Application to Rio de Janeiro. *Eng. Geol.* **2003**, *69*, 99–108. [CrossRef]

59. Gonzalez, C. *Estudio de Áreas de Riesgo Geomorfológico de La Zona Urbana y de Expansión de La Comuna de San Antonio*; Universidad de Chile: Santiago, Chile, 2005.

60. Brito, J.L. *San Antonio: Nuevas Crónicas Para Su Historia y Geografía*; Sales. Impr.: San Antonio, TX, USA, 2019.

61. Kawagoe, S.; Kazama, S.; Sarukkalige, P.R. Probabilistic Modelling of Rainfall Induced Landslide Hazard Assessment. *Hydrol. Earth Syst. Sci.* **2010**, *14*, 1047–1061. [CrossRef]

62. Heintz, J.; Mahoney, M. *Guidelines For Design Of Structures For Vertical Evacuation From Tsunamis*; FEMA: Washington, DC, USA, 2008.

63. Okada, Y. Surface Deformation Due to Shear and Tensile Faults in a Half-Space. *Bull. Seismol. Soc. Am.* **1985**, *75*, 1135–1154.

64. DIHA. *Propagación Regional de Tsunamis Basados En Eventos Históricos*; DIHA: Santiago, Chile, 2011.

65. PRDW-AV. *Estudio de La Propagación Regional de Tsunamis Basados En El Evento de 1730*; PRDW-AV: Santiago, Chile, 2011.

66. Mader, C.L. *Numerical Modeling of Water Waves*; CRC Press: Boca Ratón, FL, USA, 2004.

67. Marche, F. Derivation of a New Two-Dimensional Viscous Shallow Water Model with Varying Topography, Bottom Friction and Capillary Effects. *Eur. J. Mech.* **2007**, *26*, 49–63. [CrossRef]

68. Guerra, M.; Cienfuegos, R.; Escauriaza, C.; Marche, F.; Galaz, J. Modeling Rapid Flood Propagation over Natural Terrains Using a Well-Balanced Scheme. *J. Hydraul. Eng.* **2014**, *140*, 4014026. [CrossRef]

69. Cienfuegos, R.; Barthélemy, E.; Bonneton, P. A Fourth-order Compact Finite Volume Scheme for Fully Nonlinear and Weakly Dispersive Boussinesq-type Equations. Part II: Boundary Conditions and Validation. *Int. J. Numer. Methods Fluids* **2007**, *53*, 1423–1455. [CrossRef]

70. Kotani, M. Tsunami Run-up Simulation and Damage Estimation Using GIS. *Proc. Coast. Eng. JSCE* **1998**, *45*, 356–360.

71. Walsh, T.J.; Titov, V.V.; Venturato, A.J.; Mofjeld, H.O.; Gonzalez, F.I. Tsunami Hazard Map of the Elliott Bay Area, Seattle, Washington: Modeled Tsunami Inundation from a Seattle Fault Earthquake. *Wash. Div. Geol. Earth Resour. Open File Rep.* **2003**, *14*.

72. Johnson, L.R.; Silva, W. The Effects of Unconsolidated Sediments upon the Ground Motion during Local Earthquakes. *Bull. Seismol. Soc. Am.* **1981**, *71*, 127–142.

73. Pilz, M.; Parolai, S.; Picozzi, M.; Zschau, J. Evaluation of Proxies for Seismic Site Conditions in Large Urban Areas: The Example of Santiago de Chile. *Phys. Chem. Earth Parts A/B/C* **2011**, *36*, 1259–1266. [CrossRef]

74. Code, P. *Eurocode 8: Design of Structures for Earthquake Resistance-Part 1: General Rules, Seismic Actions and Rules for Buildings*; European Committee for Standardization: Brussels, Belgium, 2005.

75. Ciurean, R.L.; Schroter, D.; Glade, T. Conceptual Frameworks of Vulnerability Assessments for Natural Disasters Reduction. In *Approaches to Disaster Management-Examining the Implications of Hazards, Emergencies and Disasters*; InTech: London, UK, 2013.

76. Guillard-Gonçalves, C.; Zêzere, J. Combining Social Vulnerability and Physical Vulnerability to Analyse Landslide Risk at the Municipal Scale. *Geosciences* **2018**, *8*, 294. [CrossRef]

77. UNESCO-RAPCA. *Introduction to the UNESCO-RAPCA Project*; ITC: Enschede, The Netherlands, 2000.

78. Susman, P.; O'Keefe, P.; Wisner, B. Global Disasters, a Radical Interpretation. *Interpret. Calam.* **1983**, 263–283.

79. Hewitt, K. *Regions of Risk: A Geographical Introduction to Disasters*; Routledge: London, UK, 2014.

80. Thywissen, K. *Components of Risk: A Comparative Glossary*; UNU-EHS: Bonn, Germany, 2006.

81. SUBDERE. *Guía Análisis de Riesgos Naturales Para El Ordenamiento Territorial*; SUBDERE: Santiago, Chile, 2011.

82. FADEU-UC. *Estudio de Riesgo de Sismos y Maremoto Para Comunas Costeras de Las Regiones de O'Higgins y Del Maule*; FADEU-UC: Providencia, Chile, 2012.

83. Marzocchi, W.; Garcia-Aristizabal, A.; Gasparini, P.; Mastellone, M.L.; Di Ruocco, A. Basic Principles of Multi-Risk Assessment: A Case Study in Italy. *Nat. Hazards* **2012**, *62*, 551–573. [CrossRef]

84. ICPR. *Non Structural Flood Plain Management: Measures and Their Effectiveness*; International Commission for the Protection of the Rhine (ICPR): Koblenz, Germany, 2002.

85. Johnstone, W.M.; Lence, B.J. Use of Flood, Loss, and Evacuation Models to Assess Exposure and Improve a Community Tsunami Response Plan: Vancouver Island. *Nat. Hazards Rev.* **2011**, *13*, 162–171. [CrossRef]

86. Vargas, G.; Farías, M.; Carretier, S.; Tassara, A.; Baize, S.; Melnick, D. Coastal Uplift and Tsunami Effects Associated to the 2010 Mw8. 8 Maule Earthquake in Central Chile. *Andean Geol.* **2011**, *38*, 219–238.

87. UNESCO. *Preparación Para Casos de Tsunami. Guía Informativa Para Los Planificadores Especializados En Medidas de Contingencia Ante Catástrofes*; UNESCO: Paris, France, 2008.

88. FEMA. *Seismic Performance Assessment of Buildings (Volume 1—Methodology)*; FEMA P-58; Federal Emergency Management Agency: Washington, DC, USA, 2012.